Saudi Pharmaceutical Journal 31 (2023) 911–920

HOSTED BY

Contents lists available at ScienceDirect

Saudi Pharmaceutical Journal

journal homepage: www.sciencedirect.com

Original article

Biosynthesis of silver nanoparticles (Ag-NPs) using *Senna alexandrina* grown in Saudi Arabia and their bioactivity against multidrug-resistant pathogens and cancer cells

Naiyf S. Alharbi, Jamal M. Khaled *, Khaled Alanazi, Shine Kadaikunnan, Ahmed S. Alobaidi

Department of Botany and Microbiology, College of Science, King Saud University, P.O. Box 2455, Riyadh 11451, Saudi Arabia

ARTICLE INFO

Article history:
Received 8 March 2023
Accepted 14 April 2023
Available online 20 April 2023

Keywords:
S. alexandrina
Silver nanoparticles (Ag-NPs)
Antibacterial Activities
Anticancer potential
Multidrug-resistant pathogens (MDRPs)

ABSTRACT

There is no doubt that the risk of drug-resistant pathogens and cancer diseases is on the rise. So, the goal of this study was to find out how effective silver nanoparticles (Ag-NPs) made by *Senna alexandrina* are at fighting these threats. In this work, *S. alexandrina* collected from Medina, Saudi Arabia was used and the biosynthesis method was applied to produce the Ag-NPs. The characterization of Ag-NPs was done using different analytical techniques, including UV spectroscopy, FT-IR, TEM, and XRD analysis. The MIC, MBC, and MTT protocols were applied to confirm the bioactivity of the Ag-NPs as antibacterial and anticancer bioagents. The findings reported indicating that the aqueous extract of *S. alexandrina* leaves, grown naturally in Saudi Arabia, is ideal for the production of bioactive Ag-NPs. The hydroxyl, aliphatic, alkene, N–H bend of primary amines, C–H bonds, and C-O bonds of alcohol were detected in this product. The small, sphere-shaped particles (4–7 nm) were the most prevalent among the bioactive Ag-NPs produced in this work. These nanoparticles inhibited some important multidrug-resistant pathogens (MDRPs) (*Escherichia coli*, *Acinetobacter baumanii/haemolyticus*, *Staphylococcus epidermidis*, and Methicillin-resistant *Staphylococcus aureus* (MRSA)), as well as their ability to inhibit breast cancer cells (MCF-7 cells). The MIC of Ag-NPs ranged from 0.03 to 0.6 mg/mL, while their MBC ranged from 0.06 to 2.5 mg/mL. Anticancer activity test showed that IC_{50} of the Ag-NPs against tested breast cancer cells was 61.9 ± 3. 8 μg/mL. According to the current results, biosynthesis using *S. alexandrina* leaves grown naturally in Saudi Arabia was an ideal technique for producing bioactive Ag-NPs that could be used to combat a variety of MDRPs and cancer diseases.

1. Introduction

Infections brought on by bacteria and other microbes that can harm humans are prevented and treated with antibiotics. One of the most significant medical advancements was the discovery of antibiotics (Nicolaou et al., 2018). Clinical Staphylococcus aureus isolates with penicillin resistance have been reported shortly after penicillin became widely available (Lobanovska et al., 2017). Several studies have shown that the widespread administration of antibacterial drugs has resulted in the emergence of drug-resistant bacterial strains (Wang et al., 2017). Antibiotics are simple to obtain and effective against many bacteria that are dangerous to people. Fleming did, however, caution us not to rely too heavily on antibiotics in the speech he made upon receiving the Nobel Prize in 1945. He was concerned about the improper use of penicillin and the easiness with which resistance could arise from inadequate treatment dosages (Browne et al., 2020).

The creation, characterization, and application of formations, devices, and systems at the nanoscale (1 nm to 100 nm) level is referred to as nanotechnology. It is a brand-new area for creating cutting-edge research and materials with numerous uses in science and technology. Nanoparticles are made with distinctive properties that attract to biologists and material scientists. Among various nanoparticles, Ag-NPs have become one of the most popular study topics in recent years (Yin et al., 2020; Aslam et al., 2021; Khuda et al., 2022).

* Corresponding author.
E-mail addresses: nalharbi1@ksu.edu.sa (N.S. Alharbi), gkhaled@ksu.edu.sa (J.M. Khaled), 438105303@student.ksu.edu.sa (K. Alanazi), sshine@ksu.edu.sa (S. Kadaikunnan), ahalobaidi@ksu.edu.sa (A.S. Alobaidi).

Peer review under responsibility of King Saud University.

ELSEVIER Production and hosting by Elsevier

https://doi.org/10.1016/j.jsps.2023.04.015
1319-0164/

The issue of bacterial resistance is getting worse, but scientists are investigating a few active antibiotics that might be able to combat bacteria that are resistant to multi-standard drugs. Gould et al. (2013) reported that the fact that some infections can't be cured is a scary sign that antibiotics are being used too much and for the wrong reasons. The question is "Could nanoparticles replace antibiotics in the face of the threat of antibiotic resistance?". It is now understood that nanotechnology can be used to treat bacterial infections (Wang et al. 2017). Silver nanoparticles are biological agents capable of combating pathogenic microorganisms. This has been demonstrated. And that its application is not confined to the medical field, but also to the environment, agriculture, food, and industry (Das et al., 2020). The findings of Jadhav et al. (2018) suggest that plant-mediated green synthetic silver nanoparticles could be promising anticancer agents that avoid the drawbacks of traditional cancer chemotherapeutic agents. Based on the concentrations tested, Ag-NPs have a strong anti-cancer effect. Nanoparticles (NPs) are important in the field of prescribed drugs due to their potent bioactivity against cancer cells. Given the significance of this fundamental concept, there is an urgent need for continued research, production, and characterization of these particles to combat cancer cells (Patil & Kim, 2017).

The green method is the best way to synthesize nanoparticles because it is less expensive and can be used for a large amount of nanoparticle synthesis (Elsharkawy, 2018). Another advantage is that this biotechnology is simple, environmentally friendly, and relatively reproducible, and the nanoparticles produced using this method are frequently more stable (Ahmed et al., 2016b). *Senna alexandrina* Mill. (Leguminosae) is found in the wild in Saudi Arabia, Yemen, and Egypt, and it is also extensively grown in Pakistan. This herb has been used in traditional medicine to treat cholera, liver diseases, constipation, typhoid, and a variety of other ailments (Ahmed et al., 2016a, 2016b).

In order to address the risks of microbial resistance to antibiotics and cancerous diseases, this work aimed to produce bioactive Ag-NPs (antibacterial and anticancer agents) using biosynthesis methods. The objectives of this work include silver nanoparticle biosynthesis using *S. alexandrina*, characterization of these particles using an ultraviolet (UV) spectrophotometer, a Fourier transform infrared spectrophotometer (FT-IR), a transmission electron microscope (TEM), and X-ray diffraction analysis, and evaluation of the biological activity of synthesized Ag-NPs as an antibacterial and anticancer bio-product.

2. Methodology

2.1. Sample collection

S. alexandrina fresh samples were collected from the Hijaz area (Medina) (24.470901 and 39.612236, latitude and longitude respectively). This city is located in Saudi Arabia with the GPS coordinates of 24° 28′ 15.2436'' N and 39° 36′ 44.0496'' E. according to https://www.latlong.net/place/medina-saudi-arabia-2246.html. The plant samples were identified by a botanist in the herbarium of the Department of Botany and Microbiology, King Saud University (KSU), Riyadh. The fresh leaves were thoroughly washed with tap water, then Mili Q water, before being used in the synthesis of silver nanoparticles. The washed plants were dried in the shade, ground into a fine powder, and stored in airtight bottles until they were used in the biosynthesis of silver nanoparticles.

2.2. Preparation of the leaves extract

Ten grams of powdered leaves were combined into 100 mL of deionized water and boiled for 30 min on a hot magnetic stirrer at 60 °C. The aqueous extract was clarified using filter paper (Whatman No. 1) after cooling (Swarnavalli et al., 2017). The clear supernatant obtained from the filtration stage was settled at 7 ± 1 °C for 4 h before collecting the top clear part and discarding the sediment part. The aqueous extract was kept at 4 ± 1 °C for further tests.

2.3. Biosynthesis of nanoparticles

Silver nitrate was used to create silver nanoparticles using the aqueous extract of *S. alexandrina* leaves obtained in the preceding stage was used. To produce the nanoparticles, different metal (silver nitrate) solutions were prepared in an Erlenmeyer flask in different concentrations (1,2,3,4,5,6,7,8,9 and 10 mM). To determine the best method for producing nanoparticles, the extract was mixed with the metals in various amounts, concentrations, RPMs, light, dark, and temperature conditions. The primary experiments revealed that the best conditions for producing Ag-NPs were the extract of metal (3:7 ratio), 220 rpm, 24 ± 1 °C, and light sun for 10 min.

The colloidal suspension of the prepared nanoparticles was centrifuged at 21380 × g and 4 ± 1 °C for 15 min at the end of the process, and the products were washed three times with sterile distilled water to remove any free metals and plant extract. A color change indicated the production of nanoparticles (a dark brown color indicates the completion of the chemical reduction process and biosynthesis of silver nanoparticles) (Al-Otibi et al., 2021).

2.4. Characterization of the biosynthesized nanoparticles

Various analytical procedures were applied to characterize the nanoparticles biosynthesized in this work. The UV-analysis was done to approve the formation and stability of produced nanoparticles. The absorbance (O.D) spectrum (202 to 800 nm) of the colloidal product was analyzed using Ultraviolet–Visible spectroscopy (Shimadzu UV-2600). The FT-IR was used to characterize surface chemistry and detect organic functional groups (e.g., carbonyls, hydroxyls). The wavelength (4000 to 400 cm-1) and spectra of emission were rescored using FTIR Spectrophotometer (VERTEX 70/70v). The powder XRD analytical technique was used to identify the phase and crystalline material of the nanoparticles. The diffraction of X-ray was done using X'Pert PRO diffractometers (Cu X-ray emitter with a wavelength of 1.5406 A° and a voltage of 40 kV). The TEM was applied to distinguish the morphology of the produced nanoparticles. The solution of Ag-NPs was diluted, and a drop of this dilution was added to the gird of TEM. The dehydration was performed, and then the TEM analysis was done using Mic, HV, and Mag JEM 1011, 80 kV, and 40000, respectively (Mittal et al., 2013; Barbhuiya et al., 2022).

2.5. Antibacterial activity

The bioactivity of the biosynthesized nanoparticles as antibacterial agents was evaluated using multidrug-resistant human pathogenic bacteria (*Escherichia coli*, *Acinetobacter baumanii/haemolyticus*, *Staphylococcus epidermidis*, and MRSA). All of these microbes are reference strains available at Microbiological Laboratory, Botany and Microbiology Department, College of Science, King Saud University. Susceptible testing for all these microbial strains using the Vitek System (bioMérieux) showed that these microbial strains were resistant to multidrug (Tables 1 and 2). The standard macro-broth dilution assay was applied to calculate the minimum inhibitory concentration (MIC) and minimum bactericidal concentration (MBC). MIC is the lowest concentration of the antibacterial agent that inhibits visible bacterial growth, whereas MBC is the lowest concentration at which bacteria can no longer

Table 1
MIC of standard antibiotics against *S. epidermidis* and MRSA strains tested in this work using Vitek System (Biomerieux, France).

S. epidermidis			MRSA		
Antibiotics	MIC*		Antibiotics	MIC*	
Gentamicin-Syn	> 500		Amox/k Clav	<=4/2	R
Gentamicin	> 8	R	Ampicillin	8	BLAC
Imipenem	> 8	R	Cefoxitin Screen	> 4	POS
Cefoxitin	> 8	R	Ciprofloxacin	<=1	S
Cefotaxime	> 32	R	Clindamycin	0.5	
Ampicillin	X	R	Erythromycin	> 4	
Penicillin G	> 0.25	R	Fosfomycin	<=32	S
Oxacillin	> 2	R	Fusidic Acid	16	I
Amoxicillin-clavulanate	> 4/2	R	Gentamicin	<=1	S
Daptomycin	<=1	S	Imipenem	<=4	R
Trimethoprim-sulfamethoxazole	Apr-76	R	Levofloxacin	<=1	S
Teicoplanin	<=2	S	Linezolid	<=2	S
Vancomycin	1	S	Mupirocin	<=4	S
Clindamycin	> 2	R	Nitrofurantoin	<=32	S
Erythromycin	> 4	R	Oxacillin	> 2	R
Fusidic Acid	8		Penicillin	8	BLAC
Linezolid	2	S	Tetracycline	<=4	S
Mupirocin High Level	> 256	R	Trimeth/Sulfa	<=2/38	S
Nitrofurantoin	32	S	Vancomycin	4	I
Ciprofloxacin	> 2	R			
Moxifloxacin	2	S			
Rifampin	<=0.5	S			
Tetracycline	8	I			

* I = Intermediate, R = Resistant, MIC = mcg/ml (mg/l), POS = Positive, NEG = Negative and Blac = Beta-lactamase positive.

Table 2
MIC of standard antibiotics against *E. coli* and *A. baumannii/haemolyticus* strains tested in this work using Vitek System (Biomerieux, France).

E. coli			*A. baumannii/haemolyticus*		
Antibiotic	MIC*		Antibiotic	MIC*	
Amikacin	<=16	S	Amikacin	> 32	R
Amox/k Clav	> 16/8	R	Amox/k Clav	> 16/8	
Ampicillin	> 16	R	Ampicillin	> 16	
Cefazolin	> 16	R	Cefazolin	> 16	
Cefepime	<=8	S	Cefepime	> 16	R
Cefotaxime	> 32	R	Cefotaxime	> 32	R
Cefoxitin	> 8	R	Cefoxitin	> 8	
Ceftazidime	> 16	R	Ceftazidime	> 16	R
Cefuroxime	> 16	R	Cefuroxime	> 16	
Ciprofloxacin	> 2	R	Clprofloxacin	> 2	R
Collstin	<=2		Colistin	<=2	S
Fosfomycin	<=32	S	Fosfomycin	> 32	
Gentamicin	<=4	S	Gentamicin	> 8	R
Imipenem	<=4	S	Imipenem	> 8	R
Levofloxacin	> 4	R	Levofloxacin	> 4	R
Meropenem	<=1	S	Meropenem	> 8	R
Nitrofurantoin	<=32		Nitrofurantoin	> 64	
Norfloxacin	> 8		Norfloxacin	> 8	
Pip/Tazo	64	I	Tetracycline	> 8	R
Tetracycline	> 8	R	Tobramycin	> 8	R
Tigecycline	<=1	S	Trimeth/Sulfa	<=2/38	S
Tobramycin	> 8	R	Tigecycline		S
Trimeth/Sulfa	> 2/38	R			

*S = Susceptible,, I = Intermediate, R = Resistant, MIC = mcg/ml (mg/l), POS = Positive, NEG = Negative and Blac = Beta-lactamase positive

grow at all (Elshikh et al., 2016; Ghaedi et al., 2015). Control groups in this experiment were chloramphenicol as the positive control group and sterile normal saline as the negative control group. This method used sterile distilled water to create a stock solution containing 1.3 mg/mL of Ag-NPs. Ten test tubes were prepared for each microbe, with each receiving 900 μL of sterile nutrient broth (Oxoid, UK) and 100 μL of microbial suspension (10^5 microbial cell/mL). The microbial suspension was made from pure colonies and had an optical density of 0.60 at 550 nm. The first of eight test tubes received 1 mL of Ag-NPs solution and was thoroughly mixed; 1 mL was then transferred from this test tube to the following tube. This procedure was repeated until the eighth test tube was reached, at which point 1 mL of the last test tube was discarded. The standard antibiotic was subjected to the same procedures. The ninth and tenth test tubes were treated with sterile normal saline and leaven, respectively. The incubation of the test tubes was done aerobically at 37 ± 1 °C for 20 h, and the absence of microbial growth was confirmed using turbidity measurements at 550 nm and the sub-cultivation method.

2.6. Anticancer activity of nanoparticles

The cultivation of human breast cancer cells (MCF-7) (Thermo Fisher Scientific Inc. UK) was performed at 37 ± 1 °C and 5% CO_2

using anaerobic incubator. The medium used in this test contained 10% fetal bovine serum (FBS). For 24 h, the cells ($5X10^4$ cells/well) were plated onto 24-well plates. The cancer cells were then exposed to the nanoparticles at concentrations of 100, 50, 25, and 12.5 mg/ml and incubated for 48 h. After that, each well was treated with 100 µL of chemical reagent (5 mg/ml of MTT) and incubated for 2 h at 37 ± 1 °C using the CO_2 incubator. According to Sankar et al. (2013), the formazan that formed during the previous treatment was dissolved in 1 mL of acidified isopropanol. Then, the optical density (OD) was measured at 540 nm with a microplate reader (BioTek, USA). The percentage of cell viability was determined as follows:

% Viable cells = [Average OD of treated MCF-7/ Average OD of untreated MCF-7] × 100.

The concentration of nanoparticles that caused 50% inhibition (IC_{50}) was determined using the dose response curve of the percentage of living cells.

2.7. Design of the experiment and statistical analysis

The present investigation used a completely randomized design (CRD). This design tested all extractions and products equally likely. The results' means and standard deviations were calculated, and the data was analyzed in SPSS using post hoc test in one-way ANOVA (IBM SPSS Statistics, version 25, USA).

3. Results

The main goals of this study were to synthesize Ag-NPs from the leaves of *S. alexandrina* grown in Saudi Arabia and evaluate their biological activity as antibacterial and anticancer agents.

3.1. Biosynthesis of silver nanoparticles

The results shown in Fig. 1 demonstrate an alteration in the color of the reaction mixture, which contained *S. alexandrina* leaves extract and silver nitrate. After 10 min of exposure to sunlight, the color of the reaction mixture changed from golden yellow to dark brown, indicating that the silver salts were reduced into silver ions.

3.2. UV–spectrophotometer

UV–visible spectral analysis confirmed the formation of Ag-NPs. The spectral analysis revealed the highest absorbance at 490 nm, indicating that silver nitrate (Ag +) was successfully converted to silver nanoparticles. Fig. 2 shows that the wavelength range extends from 426 to 668 nm, with 490 nm being the optimum.

3.3. FT-IR analysis

The FT-IR spectrum analysis of Ag-NPs biosynthesized using *S. alexandrina* aqueous leaves extract revealed eight peaks (Fig. 3), including a broad peak at around 3205.79 cm-1, most likely for hydroxyl groups O–H stretch vibration. The aliphatic C–H symmetry stretching vibration was most likely represented by a weak peak at 2918.79 cm-1. A strong peak at 1630.80 cm-1 was most likely caused by C = C stretching and N–H bending of primary amines, and two other peaks at 1450.48 cm-1 and 1385.34 cm-1 were also caused by C–H bending. Some peaks in the finger print region at 1260.29 cm-1 and 1069.92 cm-1 could be attributed to alcohol C-O stretching. The last broad peak was at 599.73 cm-1, which is attributed to the Ag-NPs indicated by the arrow.

Table 3 displays the different characteristic functional groups of *S. alexandrina* extract as determined by the FT-IR spectrum. The data reported that the extract produced from *S. alexandrina* contains several functional groups, including normal "polymeric" OH, Methylene C–H, Alkenyl C = C, Methyl C–H, Trimethyl or "tert-butyl", Aromatic ethers, aryl -O, Alkyl-substituted ether, C-O, Aromatic ethers, aryl -O, Alkyl-substituted ether, and C-O. The stretching vibration was recorded for four functional groups (normal"polymeric" OH, Alkenyl C = C, Aromatic ethers, aryl -O, Alkyl-substituted ether, C-O, Aromatic ethers, aryl -O, Alkyl-substituted ether, C-O, Aromatic ethers, aryl -O, Alkyl-substituted ether, C (Methylene CH and Methyl CH).

3.4. XRD analysis

The crystalline structure of silver nanoparticles was revealed by XRD analysis of powdered Ag-NPs biosynthesized using *S. alexandrina* leaves extract. Fig. 4 shows four intense peaks at angles (2θ) 32.01, 38.1, 46.08, and 64.3°, corresponding to the planes (101), (111), (200), and (220), respectively.

3.5. TEM analysis

According to TEM analysis, the Ag-NPs biosynthesized using *S. alexandrina* leaves extract have a spherical shape with sizes ranging from 4 to 20 nm, as shown in Fig. 5. Small particles with sizes ranging from 4 to 7 nm had the greatest distribution and frequency.

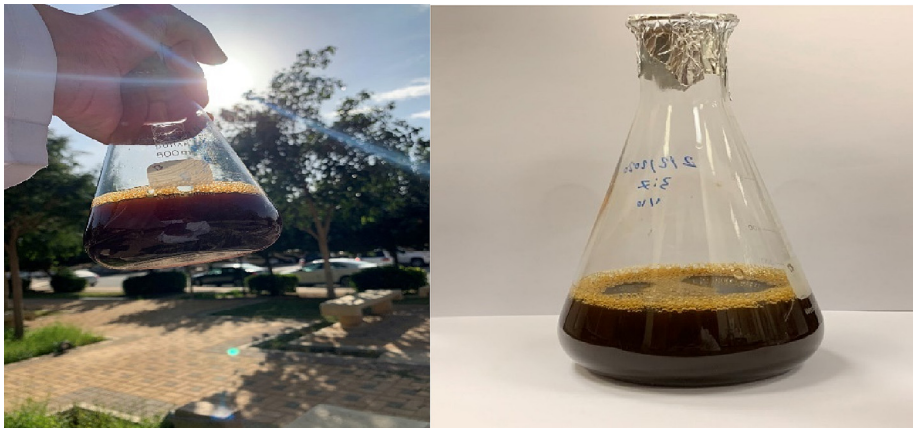

Fig. 1. *S. alexandrina* leaves extract treated with silver nitrate after 10 min of exposure to sunlight. The dark brown color indicates that the chemical reduction process has been completed.

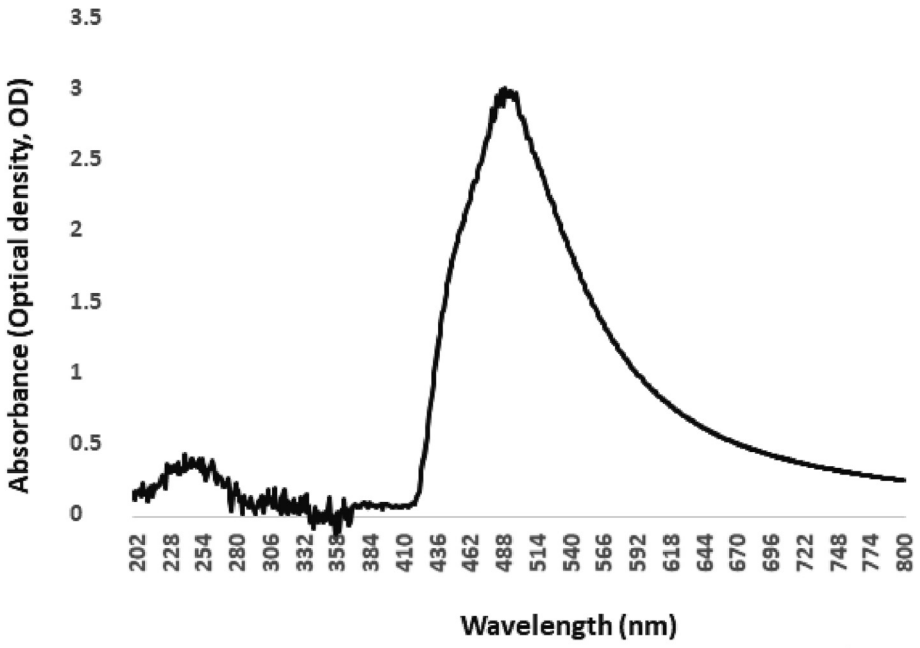

Fig. 2. UV–spectrophotometer analysis of Ag-NPs biosynthesized using aqueous leaves extract of *S. alexandrina.*

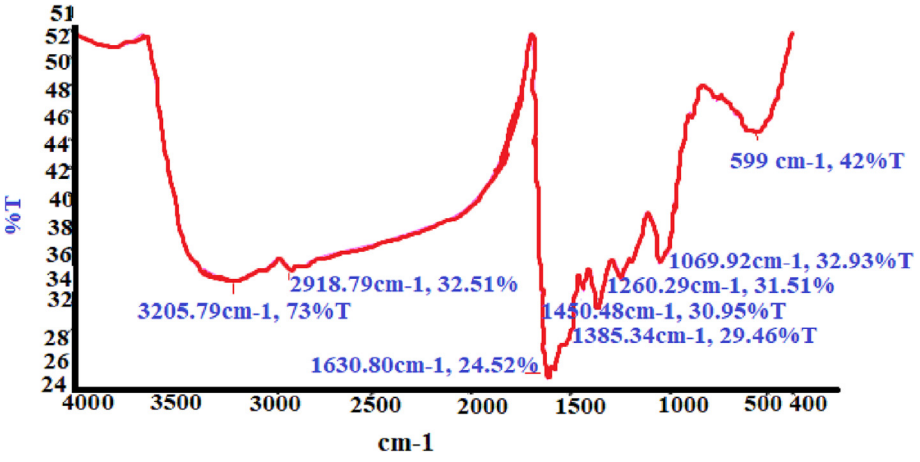

Fig. 3. FT-IR analysis of the biosynthesized Ag-NPs using aqueous leaves extract of *S. alexandrina.*

Table 3
The FT-IR spectrum used to identify the various functional groups of aqueous leaves extract of *S. alexandrina.*

Wavenumber (CM-1)	Functional group
3400–3200 (3205.79)	Normal "polymeric" OH stretch
2935–2915 (2918.79)	Methylene C–H asym.
1680–1630 (1630.80)	Alkenyl C = C stretch
1470–1430 (1450.48)	Methyl C–H asym.
1395–1385 (1385.34)	Trimethyl or "tert-butyl" (multiplet)
1270–1230 (1260.29)	Aromatic ethers, aryl -O stretch
1150–1050 (1069.92)	Alkyl-substituted ether, C-O stretch

3.6. MIC and MBC results

Ag-NPs obtained in this experiment were tested for antibacterial activity against MDRPs (MRSA, *S. epidermidis*, *E. coli*, and *A. baumanii*/*haemolyticus*). The findings were compared to those obtained with the standard antibiotic (Chloramphenicol). Figs. 6 and 7 show that the MIC of Ag-NPs was between 0.3 and 0.6 mg/mL, while the MBC of Ag-NPs was between 0.6 and 2.5 mg/mL. Except for *Acinetobacter* sp., which showed high resistance to the antibiotic when compared to Ag-NPs, the MICs of Ag-NPs against all tested microbial pathogens were higher than the MICs of the standard antibiotic. When compared to all other treatments, the MBC of Ag-NPs against MRSA was significantly different ($P < 0.05$). According to the one-way ANOVA analysis, the MBCs of Ag-NPs and the antibiotic are significantly different ($P < 0.05$).

3.7. Anticancer activity of nanoparticles

To assess the cytotoxic activity of Ag-NPs synthesized in this study using *S. alexandrina* leaves extract, MCF-7 cells were given various doses (0, 12.5, 25, 50, and 100 µg/mL). Lower doses of Ag-NPs (12.5 and 25 µg/mL) did not show significant cytotoxicity

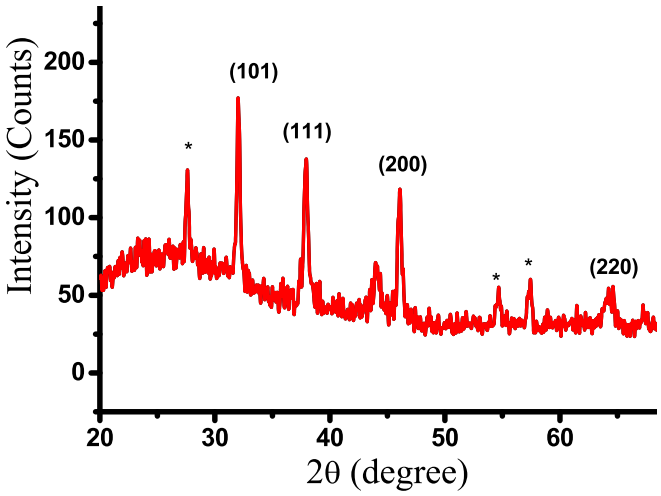

Fig. 4. XRD analysis of Ag-NPs produced using *S. alexandrina* leaves extract.

against MCF-7, according to the findings. However, at the highest concentration of 100 µg/mL, Ag-NPs demonstrated exceptional cytotoxicity (Fig. 8). The IC_{50} value of Ag-NPs was calculated to be 61.93.8 µg/mL when tested against MCF-7.

4. Discussion

Many studies have shown that the spread and misuse of antibacterial drugs has resulted in the rise of bacterial strains that are resistant to many standard drugs since the discovery of the first antibiotic. Many studies were conducted on this topic when antibiotic-resistant microbes became prevalent and a threat to human society. Ag-NPs are created for a variety of reasons, one of which is that numerous scientific studies on Ag-NPs have revealed that they have powerful antibacterial and anticancer properties. The current research aimed to biosynthesize Ag-NPs from aqueous leaves extract of *S. alexandrina* grown in Saudi Arabia. Analytical techniques such as FT-IR, UV spectrophotometer, XRD, and TEM were used to characterize biosynthesized Ag-NPs. This product's biological activity as an antibacterial and anticancer agent was also assessed.

Green synthesis of nanoparticles is widely accepted as the best method for producing nanoparticles because it is environmentally friendly and uses naturally renewable resources. Actually, this is one of the few agreed-upon facts about nanoparticle production. Initially, the method was developed to produce more biocompatible Ag-NPs than those produced chemically and to avoid cytotoxicity tests, which are required in chemical assay production (Agarwal et al., 2017; Kaur & Sidhu, 2021).

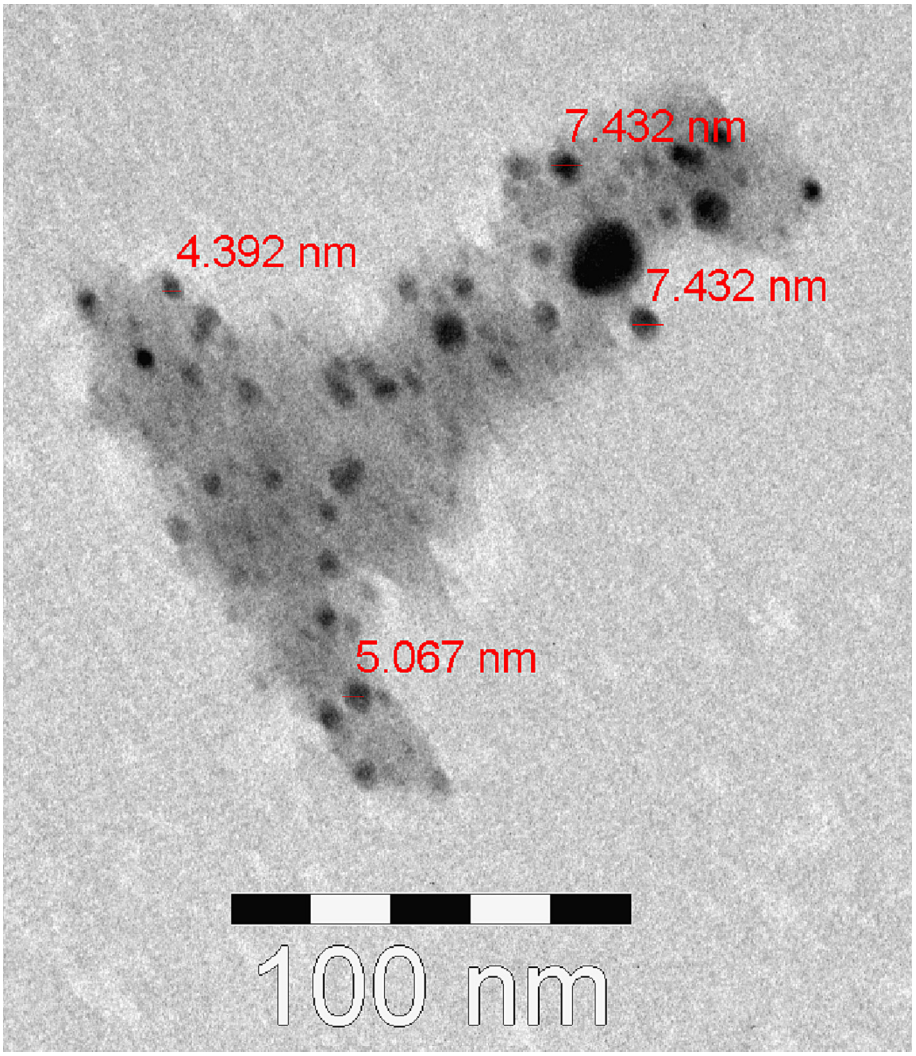

Fig. 5. TEM image of Ag-NPs shows that the size of biosynthesized Ag-NPs using *S. alexandrina* extract ranged between 4 and 20 nm.

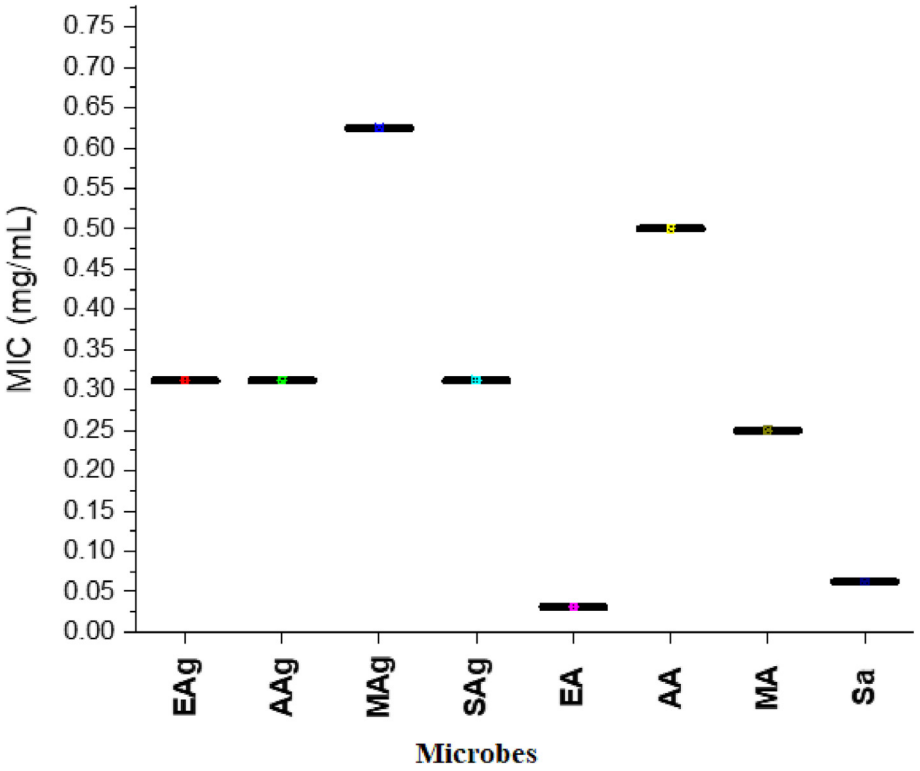

Fig. 6. Minimum inhibitory concentration (MIC) of Ag-NPs and standard antibiotics (Chloramphenicol) against against *E. coli*, *Acinetobacter* sp, MRSA and *S. epidermidis*. EAg = *E. coli* treated with Ag-NPs, AAg = *Acinetobacter* treated with Ag-NPs, MAg = MRSA treated with Ag-NPs, SAg = *S. epidermidis* treated with Ag-NPs, EA = *E. coli* treated with antibiotic, AA = *Acinetobacter* treated with antibiotic, MA = MRSA treated with antibiotic, and SA = *S. epidermidis* treated antibiotic. * Standard error was zero where the three replicates of MICs had the same value.

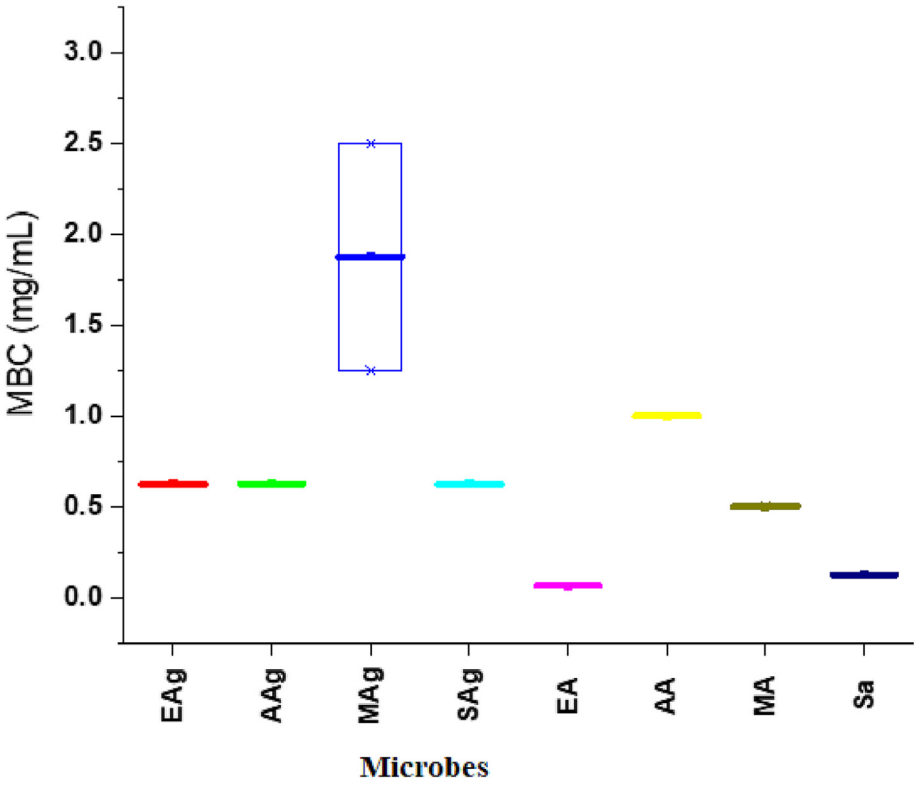

Fig. 7. The minimum bactericidal concentration (MBC) of Ag-NPs and standard antibiotics (Chloramphenicol) against against *E. coli*, *Acinetobacter* sp, MRSA and *S. epidermidis*. EAg = *E. coli* treated with Ag-NPs, AAg = *Acinetobacter* treated with Ag-NPs, MAg = MRSA treated with Ag-NPs, SAg = *S. epidermidis* treated with Ag-NPs, EA = *E. coli* treated with antibiotic, AA = *Acinetobacter* treated with antibiotic, MA = MRSA treated with antibiotic, and SA = *S. epidermidis* treated antibiotic.

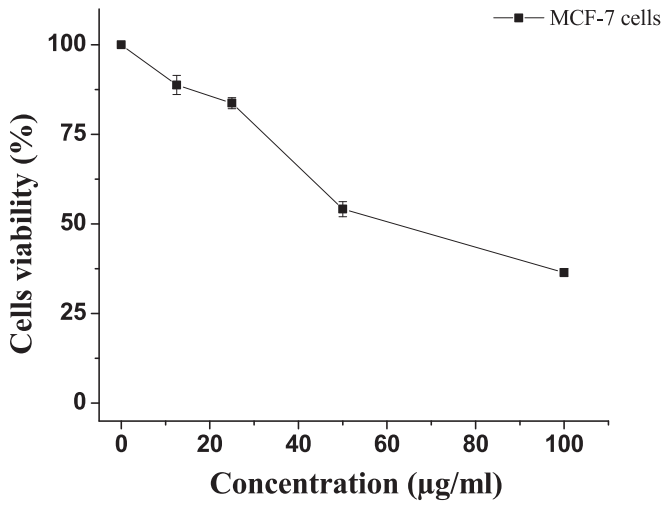

Fig. 8. The effect of Ag-NPs biosynthesized using *S. alexandrina* leaves extract on the viability of MCF-7 cells. The MTT assay was used to calculate the biological activity of different concentrations of Ag-NPs on cell generation. The various Ag-NP concentrations were prepared and used to treat MCF-7 for 48 h. For triplicates, values were expressed as means ± SD.

The green synthesis of Ag-NPs is quickly demonstrated by the solution's obvious color shift to dark brown (Nahar et al., 2021). That shift in color was clearly visible in our current work. According to previous research, the biomolecules of this mixture reaction are the result of rapid silver ion reduction and Ag-NP stabilization. The current study's findings are consistent with many previous studies that produced Ag-NPs using green synthesis methods, such as *Citrus sinensis* (navel orange) peel (Khabeeri et al., 2020). Despite claims that the color change from clear to dark brown is reliable primary evidence for the biosynthesis of Ag-NPs using plant extracts, the color does not change in some production conditions, such as when Ag-NPs are made using *Hagenia abyssinica* leaf extract (Melkamu & Bitew, 2021).

UV–Vis spectroscopy was used in this study to track the evolution of Ag-NPs. At 490 nm, the absorption peak of Ag-NPs in solution was observed. The majority of the UV–Vis spectra observed were sharp, with a single peak of surface plasmon resonance (SPR) absorption, indicating a small size distribution of spherical Ag-NPs. This study backs up previous findings that the absorption spectra at 490 nm clearly characterize the appearance of Ag-NPs (Manukumar & Kumar 2017; Balachandar et al., 2019). Furthermore, the UV–Vis spectrum of Ag-NPs formation has been confirmed to be between 350 and 490 nm, with sharp peaks at 350, 380, 420, and 490 nm (Dong et al., 2021). Kuppusamy et al. (2022) reported that a spectrophotometer with visible and ultraviolet rays confirmed the composite samples, with peaks close to 490 nm recorded at 535 nm and 456 nm for gold and silver particles, respectively. In our research, we found that the wavelength range extends from 426 to 668 nm, with 490 nm being the optimal wavelength for obtaining the highest possible absorbency.

The functional groups in the leaves extract of *S. alexandrina* that could be responsible for the bioformation of Ag-NPs from silver ions were identified using FTIR analysis. The presence of functional groups such as hydroxyl, aliphatic, an alkene (C = C double bonds that are known alkenes), the N–H bend of primary amines, C–H bonds, and alcohol C-O bonds was confirmed by this analysis. According to AbdelRahim et al. (2017), the crbonyl group of amino acid residues and protein peptides may play a biochemical role in preventing Ag-NP agglomeration and stabilizing the biosynthesized Ag-NPs in the extract. It has been established that the presence of aliphatic amines in the production medium results in Ag-NPs and that this process can be carried out in the absence of carboxylic acid and amine molecules. Furthermore, Uznanski et al. (2017) reported that the stabilization of Ag-NPs is primarily dependent on the strong interaction between carboxylate and a very small amount of amine produced by the silver precursor that interacted with the carboxylic acids.

The biosynthesized Ag-NPs produced in our investigation using *S. alexandrina* extract have a spherical shape and sizes ranging from 4 to 20 nm. Small particles with sizes ranging from 4 to 7 nm were the most common and prevalent. It has been reported that one of the most important characteristics that play a significant role in cellular bio-transportation is the size of the Ag-NPs, with small Ag-NPs having a high ability to pass through the cell membrane (Mohanta et al., 2017). The size of the Ag-NPs produced by the biosynthesis assay is clearly affected by the method of preparation and the nature of the extract. Mohanta et al. (2017), for example, produced Ag-NPs using the aqueous leaves extract of *Protium serratum*, with average sizes of 74.56 0.46 nm, whereas Liu et al., (2021) produced spherical Ag-NPs ranging in size from 50 to 100 nm using yeast extracts.

The biological activity of Ag-NPs produced using *S. alexandrina* leaves extract as an antibacterial agent against MRSA, *S. epidermidis*, *E. coli*, and *A. baumanii*/*haemolyticus* varied depending on the microbial pathogens tested in this study. These nanoparticles' bioactivity against MRSA was the least effective of all the microbial pathogens tested in this work. According to numerous scientific reports, Ag-NPs are gaining traction as an alternative therapy against drug-resistant pathogens, particularly MRSA (Nanda and Saravanan, 2009; Masimen et al., 2022). MRSA strains were found to be more sensitive to biosynthesized Ag-NPs using *S. aureus* extract than methicillin-resistant *S. epidermidis*, *S. pyogenes*, *Salmonella typhi*, and *Klebsiella pneumoniae*. These differences in our findings and those studies are acceptable because the methods of production and microbial strains used in the two investigations were different. According to Hamida et al. (2020), the MICs and MBCs of D-SNPs (Ag-NPs produced using *Desertifilum* sp.) were 1.2 and 1.5 for *E. coli* and MRSA, respectively (MIC/MBC was 0.8 for both *E. coli* and MRSA). Our findings show that Ag-NPs biosynthesized from *S. alexandrina* leaves have higher biological activity as antibacterials against *E. coli* and MRSA than D-SNPs produced from *Desertifilum* sp. The scientific findings from this study and others have confirmed that biosynthesized Ag-NPs are broad-spectrum antibacterial agents because they can act on both Gram-positive and Gram-negative bacteria.

Mikhailova (2020) summarized the proposed biomechanics of Ag-NPs' influence on Gram-positive and Gram-negative bacteria. These mechanisms include influencing cell wall activity (cell-wall leakage), genetic material (interfere with DNA functioning), ribosomes (ribosome subunit destabilization), enzymes (enzyme denaturation), and the generation of reactive oxygen species. In fact, we did not investigate the mechanism of action of biosynthesized Ag-NPs using the aqueous extract of *S. alexandrina* in our current study, and we expect that the bio-mechanism is primarily acting on the microbial plasma membrane, and even though we recommend more research on this topic. In addition to antibacterial activity, the biosynthesized Ag-NPs using *S. alexandrina* leaves extract demonstrated remarkable cytotoxicity against MCF-7 cells (a human breast cancer cell line). This is not the first study to show that Ag-NPs are effective against cancer cells in laboratory experiments, but it is a confirmation of many previous studies, such as Igaz and colleagues' study (Igaz et al., 2016), which found that the synergistic action of Ag-NPs and some histone deacetylase inhibitors has potential benefits in cancer treatment protocols. Furthermore, it has been reported that several Ag-NPs biosynthesized using plant and microbial extracts have bioactivity to inhibit a variety of cancer cells, including Ag-NPs produced using *Abel-*

moschus esculentus (L.) pulp extract (Mollick et al., 2019) and *Cleome viscosa* L. fruit extract (Lakshmanan et al., 2018).

5. Conclusion

This study aimed to produce silver nanoparticles using safe nurture extract and apply it in the control of pathogens in laboratory experiments. This study aimed to produce silver nanoparticles using a safe nurture extract and apply them to the control of pathogens in laboratory experiments. The study achieved all its objectives as it produced the silver nanoparticles using an aqueous extract obtained from the leaves of *S. alexandrina* which grows naturally in Saudi Arabia. This source is a local renewable resource with a high bio-efficiency in producing Ag-NPs using the green synthesis method, which is regarded as a rapid, low-cost, and environmentally friendly method. The silver nanoparticles produced in this work demonstrated significant biological activity against MDRPs (*E. coli*, *A. baumanii/haemolyticus*, *S. epidermidis*, and MRSA) and cancer cells (MCF-7 cells). The current study concluded that the Saudi Arabian environment is a source of natural plants that could be renewable resources for extracts that could be used to produce nanoparticles using green synthesis. Aside from their numerous applications, these nanoparticles may have antibacterial and anticancer properties that could be used to combat drug-resistant pathogens and cancer diseases. In conclusion, we recommend future studies to evaluate the different extracts of *S. alexandrina* (root, stem, and flower extracts) in terms of their efficiency in producing different nanoparticles and testing these particles as antibacterial, antifungal, and antiviral, as well as against different types of cancer cells in *vivo* and *vitro* studies.

Declaration of Competing Interest

The authors declare that they have no known competing financial interests or personal relationships that could have appeared to influence the work reported in this paper.

Acknowledgment

The authors express their sincere appreciation to the Researchers Supporting Project Number (RSPD2023R679), King Saud University, Riyadh, Saudi Arabia.

References

AbdelRahim, K., Mahmoud, S.Y., Ali, A.M., Almaary, K.S., Mustafa, A.E.Z.M., Husseiny, S.M., 2017. Extracellular biosynthesis of silver nanoparticles using *Rhizopus stolonifer*. Saudi J. Biol. Sci. 24 (1), 208–216.

Agarwal, H., Kumar, S.V., Rajeshkumar, S., 2017. A review on green synthesis of zinc oxide nanoparticles–an eco-friendly approach. Resour.-Effic. Technol. 3 (4), 406–413.

Ahmed, S., Ahmad, M., Swami, B.L., Ikram, S., 2016b. A review on plants extract mediated synthesis of silver nanoparticles for antimicrobial applications: a green expertise. J. Adv. Res. 7 (1), 17–28.

Ahmed, S.I., Hayat, M.Q., Tahir, M., Mansoor, Q., Ismail, M., Keck, K., Bates, R.B., 2016a. Pharmacologically active flavonoids from the anticancer, antioxidant and antimicrobial extracts of *Cassia angustifolia* Vahl. BMC Complement. Altern. Med. 16 (1), 460.

Al-Otibi, F., Perveen, K., Al-Saif, N.A., Alharbi, R.I., Bokhari, N.A., Albasher, G., Al-Otaibi, R.M., Al-Mosa, M.A., 2021. Biosynthesis of silver nanoparticles using *Malva parviflora* and their antifungal activity. Saudi J. Biol. Sci. 28 (4), 2229–2235.

Aslam, M., Fozia, F., Gul, A., Ahmad, I., Ullah, R., Bari, A., Mothana, R.A., Hussain, H., 2021. Phyto-extract-mediated synthesis of silver nanoparticles using aqueous extract of *Sanvitalia procumbens*, and characterization, optimization and photocatalytic degradation of azo dyes Orange G and Direct Blue-15. Molecules 26 (20), 6144.

Balachandar, R., Gurumoorthy, P., Karmegam, N., Barabadi, H., Subbaiya, R., Anand, K., Boomi, P., Saravanan, M., 2019. Plant-mediated synthesis, characterization and bactericidal potential of emerging silver nanoparticles using stem extract of *Phyllanthus pinnatus*: a recent advance in phytonanotechnology. J. Clust. Sci. 30 (6), 1481–1488.

Barbhuiya, R.I., Singha, P., Asaithambi, N., Singh, S.K., 2022. Ultrasound-assisted rapid biological synthesis and characterization of silver nanoparticles using pomelo peel waste. Food Chem. 385, 132602.

Browne, K., Chakraborty, S., Chen, R., Willcox, M.D., Black, D.S., Walsh, W.R., Kumar, N., 2020. A new era of antibiotics: The clinical potential of antimicrobial peptides. Int. J. Mol. Sci. 21 (19), 7047.

Das, C.A., Kumar, V.G., Dhas, T.S., Karthick, V., Govindaraju, K., Joselin, J.M., Baalamurugan, J., 2020. Antibacterial activity of silver nanoparticles (biosynthesis): a short review on recent advances. Biocatal. Agric. Biotechnol. 27, 101593.

Dong, B., Xue, N., Mu, G., Wang, M., Xiao, Z., Dai, L., Wang, Z., Huang, D., Qian, H., Chen, W., 2021. Synthesis of monodisperse spherical Ag-NPs by ultrasound-intensified Lee-Meisel method, and quick evaluation via machine learning. Ultrason. Sonochem. 73, 105485.

Elsharkawy, E. R. (2018). Antimicrobial Activity of Silver Nanoparticles Synthesis by Green Method from Artemisia Monosperma. Oriental Journal of Chemistry, 34 (3).P.1420

Elshikh, M., Ahmed, S., Funston, S., Dunlop, P., McGaw, M., Marchant, R., Banat, I.M., 2016. Resazurin-based 96-well plate microdilution method for the determination of minimum inhibitory concentration of biosurfactants. Biotechnol. Lett. 38 (6), 1015–1019.

Ghaedi, M., Yousefinejad, M., Safarpoor, M., Khafri, H.Z., Purkait, M.K., 2015. Rosmarinus officinalis leaf extract mediated green synthesis of Ag-NP sand investigation of its antimicrobial properties. J. Ind. Eng. Chem. 31, 167–172.

Gould, I.M., Bal, A.M., 2013. New antibiotic agents in the pipeline and how they can help overcome microbial resistance. Virulence 4 (2), 185–191.

Hamida, R.S., Ali, M.A., Goda, D.A., Al-Zaban, M.I., 2020. Lethal mechanisms of nostoc-synthesized silver nanoparticles against different pathogenic bacteria. Int. J. Nanomed. 15, 10499.

Igaz, N., Kovács, D., Rázga, Z., Kónya, Z., Boros, I.M., Kiricsi, M., 2016. Modulating chromatin structure and DNA accessibility by deacetylase inhibition enhances the anti-cancer activity of silver nanoparticles. Colloids Surf. B Biointerfaces 146, 670–677.

Jadhav, K., Deore, S., Dhamecha, D., Hr, R., Jagwani, S., Jalalpure, S., Bohara, R., 2018. Phytosynthesis of silver nanoparticles: characterization, biocompatibility studies, and anticancer activity. ACS Biomater Sci. Eng. 4 (3), 892–899.

Kaur, K., Sidhu, A.K., 2021. Green synthesis: an eco-friendly route for the synthesis of iron oxide nanoparticles. Front. Nanotechnol. 3, 655062.

Khabeeri, O.M., Al-Thabaiti, S.A., Khan, Z., 2020. Citrus sinensis peel waste assisted synthesis of Ag-NPs: effect of surfactant on the nucleation and morphology. SN Appl. Sci. 2 (12), 1–15.

Khuda, F., Jamil, M., Khalil, A.A.K., Ullah, R., Ullah, N., Naureen, F., Abbas, M., Khan, M.S., Ali, S., Farooqi, H.M.U., Ahn, M.J., 2022. Assessment of antioxidant and cytotoxic potential of silver nanoparticles synthesized from root extract of *Reynoutria japonica* Houtt. Arab. J. Chem. 15, (12) 104327.

Kuppusamy, P., Kim, S., Kim, S.J., Song, K.D., 2022. Antimicrobial and cytotoxicity properties of biosynthesized gold and silver nanoparticles using D. brittonii aqueous extract. Arab. J. Chem. 15, (11) 104217.

Lakshmanan, G., Sathiyaseelan, A., Kalaichelvan, P.T., Murugesan, K., 2018. Plant-mediated synthesis of silver nanoparticles using fruit extract of *Cleome viscosa* L.: assessment of their antibacterial and anticancer activity. Karbala Int. J. Mod. Sci. 4 (1), 61–68.

Lobanovska, M., Pilla, G., 2017. Focus: drug development: Penicillin's discovery and antibiotic resistance: lessons for the future? Yale J. Biol. Med. 90 (1), 135.

Manukumar, H.M., Umesha, S., Kumar, H.N., 2017. Promising biocidal activity of thymol loaded chitosan silver nanoparticles (TC@Ag-NPs) as anti-infective agents against perilous pathogens. Int. J. Biol. Macromol. 102, 1257–1265.

Masimen, M.A.A., Harun, N.A., Maulidiani, M., Ismail, W.I.W., 2022. Overcoming methicillin-resistance *Staphylococcus aureus* (MRSA) using antimicrobial peptides-silver nanoparticles. Antibiotics 11 (7), 951.

Melkamu, W.W., Bitew, L.T., 2021. Green synthesis of silver nanoparticles using *Hagenia abyssinica* (Bruce) JF Gmel plant leaf extract and their antibacterial and anti-oxidant activities. Heliyon 7 (11), e08459.

Mikhailova, E.O., 2020. Silver nanoparticles: mechanism of action and probable bio-application. J. Funct. Biomater. 11 (4), 84.

Mittal, A.K., Chisti, Y., Banerjee, U.C., 2013. Synthesis of metallic nanoparticles using plant extracts. Biotechnol. Adv. 31 (2), 346–356.

Mohanta, Y.K., Panda, S.K., Bastia, A.K., Mohanta, T.K., 2017. Biosynthesis of silver nanoparticles from *Protium serratum* and investigation of their potential impacts on food safety and control. Front. Microbiol. 8, 626.

Mollick, M.M.R., Rana, D., Dash, S.K., Chattopadhyay, S., Bhowmick, B., Maity, D., Mondal, D., Pattanayak, S., Roy, S., Chakraborty, M., Chattopadhyay, D., 2019. Studies on green synthesized silver nanoparticles using *Abelmoschus esculentus* (L.) pulp extract having anticancer (in vitro) and antimicrobial applications. Arab. J. Chem. 12 (8), 2572–2584.

Nahar, K.N., Rahaman, M., Khan, G.M., Islam, M., Al-Reza, S.M., 2021. Green synthesis of silver nanoparticles from *Citrus sinensis* peel extract and its antibacterial potential. Asian J. Green Chem. 5 (1), 135–150.

Nanda, A., Saravanan, M., 2009. Biosynthesis of silver nanoparticles from *Staphylococcus aureus* and its antimicrobial activity against MRSA and MRSE. Nanomed. Nanotechnol. Biol. Med. 5 (4), 452–456.

Nicolaou, K.C., Rigol, S., 2018. A brief history of antibiotics and select advances in their synthesis. J. Antibiot. 71 (2), 153.

Patil, M.P., Kim, G.D., 2017. Eco-friendly approach for nanoparticles synthesis and mechanism behind antibacterial activity of silver and anticancer activity of gold nanoparticles. Appl. Microbiol. Biotechnol. 101 (1), 79–92.
Sankar, R., Karthik, A., Prabu, A., Karthik, S., Shivashangari, K.S., Ravikumar, V., 2013. Origanum vulgare mediated biosynthesis of silver nanoparticles for its antibacterial and anticancer activity. Colloids Surf. B Biointerfaces 108, 80–84.
Swarnavalli, G.C.J., Dinakaran, S., Raman, N., Jegadeesh, R., Pereira, C., 2017. Bio inspired synthesis of monodispersed silver nano particles using *Sapindus emarginatus* pericarp extract–Study of antibacterial efficacy. J. Saudi Chem. Soc. 21 (2), 172–179.
Uznanski, P., Zakrzewska, J., Favier, F., Kazmierski, S., Bryszewska, E., 2017. Synthesis and characterization of silver nanoparticles from (bis) alkylamine silver carboxylate precursors. J. Nanopart. Res. 19 (3), 1–20.
Wang, L., Hu, C., Shao, L., 2017. The antimicrobial activity of nanoparticles: present situation and prospects for the future. Int. J. Nanomed. 12, 1227–1249.
Yin, I.X., Zhang, J., Zhao, I.S., Mei, M.L., Li, Q., Chu, C.H., 2020. The antibacterial mechanism of silver nanoparticles and its application in dentistry. Int. J. Nanomed. 15, 2555–2562.